· Article ·
doi: 10.13679/j.advps.2014.4.00289

Advances in Polar Science
December 2014 Vol. 25 No. 4: 289-299

Linkages between Arctic sea ice cover, large-scale atmospheric circulation, and weather and ice conditions in the Gulf of Bothnia, Baltic Sea

Timo Vihma[1*], Bin Cheng[1], Petteri Uotila[1], WEI Lixin[1,2] & QIN Ting[2]

[1] Finnish Meteorological Institute (FMI), Helsinki, Finland;

[2] National Marine Environmental Forecasting Centre (NMEFC), Beijing 100081, China

Received 11 October 2014; accepted 20 December 2014

Abstract During years 1980/1981–2012/2013, inter-annual variations in sea ice and snow thickness in Kemi, in the northern coast of the Gulf of Bothnia, Baltic Sea, depended on the air temperature, snow fall, and rain. Inter-annual variations in the November—April mean air temperature, accumulated total precipitation, snow fall, and rain, as well as ice and snow thickness in Kemi and ice concentration in the Gulf of Bothnia correlated with inter-annual variations of the Pacific Decadal Oscillation (PDO), Arctic Oscillation (AO), North Atlantic Oscillation (NAO), Scandinavian Pattern (SCA), and Polar / Eurasian Pattern (PEU). The strong role of PDO is a new finding. In general, the relationships with PDO were approximately equally strong as those with AO, but rain and sea ice concentration were better correlated with PDO. The correlations with PDO were, however, not persistent; for a study period since 1950 the correlations were much lower. During 1980/1981—2012/2013, also the Pacific / North American Pattern (PNA) and El Nino–Southern Oscillation (ENSO) had statistical connections with the conditions in the Gulf of Bothnia, revealed by analyzing their effects combined with those of PDO and AO. A reduced autumn sea ice area in the Arctic was related to increased rain and total precipitation in the following winter in Kemi. This correlation was significant for the Pan-Arctic sea ice area in September, October, and November, and for the November sea ice area in the Barents / Kara seas.

Keywords **Arctic, Arctic Oscillation, Baltic Sea, North Atlantic Oscillation, Pacific Decadal Oscillation, precipitation, sea ice, snow**

Citation: Vihma T, Cheng B, Uotila P, et al. Linkages between Arctic sea ice cover, large-scale atmospheric circulation, and weather and ice conditions in the Gulf of Bothnia, Baltic Sea. Adv Polar Sci, 2014, 25: 289-299, doi:10.13679/j.advps.2014.4.00289

1 Introduction

The Baltic Sea is a semi-enclosed sea located in the Northern Europe (10°—30°E, 53°—66°N; Figure 1). The sea is shallow with an average depth of about 55 m, and the water is brackish with an average salinity roughly 20% of the open ocean value. In the Baltic Sea, the ice season lasts from a few weeks in the southern coast up to half a year in the northern Gulf of Bothnia. The primary motivation to study sea ice in the Baltic Sea has been related to winter navigation and, more recently, climate research. The extent and thickness of the ice cover and the duration of the ice season are important for navigation, offshore industries, fishing, and recreational use of the sea[1]. Inter-annual variations in winter weather and sea ice conditions in the Baltic Sea region are very large, which generates an interest to better understand the factors controlling these variations. Already for centuries there has been an interest to monitor the ice extent and thickness[2]. The historical sea ice extents since 1720 have been estimated[3].

The atmosphere is the primary driving force for ice conditions in the Baltic Sea; the effects of the Atlantic Ocean are reduced by the narrow, shallow straits between Sweden and Denmark in the southwestern Baltic Sea (Figure 1a). As

* Corresponding author (email: timo.vihma@fmi.fi)

the Baltic Sea is located in the transition zone between mild North-Atlantic winters and cold continental Eurasian winters (Figure 1b), the winter climate is sensitive to variations in the large-scale wind direction. The effects of weather conditions on the Baltic Sea ice cover have been studied extensively[4-13]. These studies have mostly focused on the effects of the Arctic Oscillation (AO) and North Atlantic Oscillation (NAO) on the extent and duration of the ice season.

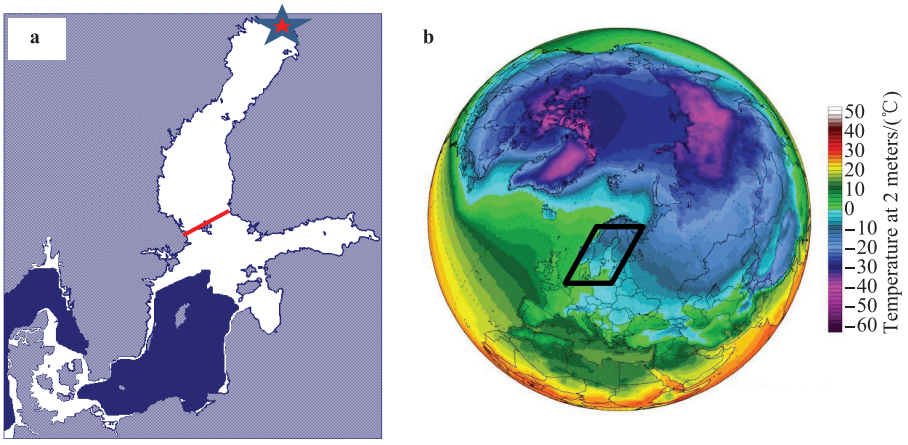

Figure 1 **a**, Map of the Baltic Sea with the study site Kemi marked by the red star. The red line marks the southern border of the Gulf of Bothnia, and the white color indicates the maximum sea ice extent in a typical winter (1995—1996); **b**, Mid-winter (December–February) mean 2-m air temperature averaged over 1980—2013. The black box approximately indicates the region shown in (a).

Only few efforts have been made to detect linkages between Baltic Sea ice cover and large-scale indices other than AO and NAO. Jevrejeva et al.[9] demonstrated that the variability of the Baltic Sea ice cover in inter-annual and decadal time scales is closely related to AO variability and, less strongly, also to the El Nino—Southern Oscillation (ENSO) variability. Other teleconnections may also be involved in the mechanisms linking the recent rapid Arctic sea ice decline with mid-latitude weather and climate[14-16]. Several studies have suggested that the effects may differ a lot between various mid-latitude regions, but none of the studies so far has focused on the Baltic Sea region.

The effects of large-scale weather conditions on sea ice thickness have received much less attention than the effects on sea ice extent in the Baltic Sea. On the basis of thickness observations Koslowski and Loewe[4] calculated the areal ice volume for small coastal areas in the southern Baltic Sea, and showed that it is negatively correlated with the NAO index. The effects of local atmospheric conditions on sea ice thickness have been addressed by several modelling studies[17-20]. The thermodynamic growth of sea ice in the Baltic Sea largely depends on the heat exchange between air and sea water, the radiative and turbulent heat fluxes at the ice/snow surface, the heat flux at the ice bottom, and the effect of precipitation[18-19]. In seasonal scale, the air temperature and precipitation are the most important thermodynamic forcing factors. The interaction of ice and snow thickness is complicated due to, among others, the two opposite effects of snow on the ice thickness: reducing the ice growth via thermal insulation and enhancing the ice growth via snow-to-ice transformation[19-21].

As a summary, previous studies have mostly focused on the effects of AO and NAO on the Baltic Sea ice cover, with little or no attention to potential effects of other globally important teleconnection patterns. These include the Pacific Decadal Oscillation (PDO), the Pacific/North American Pattern (PNA), and ENSO. In addition, there are regionally important patterns that have received relatively little attention: the Scandinavian (SCA), East Atlantic (EA), East Atlantic/West Russian (EAWR), and Polar/Eurasian (PEU) patterns.

The large-scale weather conditions related to the various indices can be characterized as follows. High positive NAO and AO indices reflect strong westerlies over the North Atlantic, which bring mild and moist maritime air over the Baltic Sea[22] and consequently delay freezing and favour ice melt. Negative NAO and AO indices are associated with a weakening or even blocking of the westerly airflow over the Atlantic Ocean, and favour a larger sea ice extent in the Baltic Sea. PDO represents the leading principal component of North Pacific (north of 20°N) monthly sea surface temperature variability. These variations affect the atmospheric pressure field; when PDO is positive, the wintertime Aleutian low is deeper and shifted southwards[23]. The teleconnections to Northern Europe are not well known (discussed in Section 4). The sea surface temperature variations associated with ENSO generate atmospheric pressure variations in the western Pacific: the warm (positive) phase of ENSO is related to a high pressure and the cold (negative) phase to a low pressure. The related teleconnections are widespread[24]. The positive phase of the PNA is associated with positive anomalies in the 500-hPa geopotential height in the regions of Hawaii and west of the Rocky Mountains and negative anomalies south of the Aleutian Islands and in the southeastern USA. During

the positive phase the East Asian jet stream is strong, whereas during the negative phase the jet stream is located further east and typically breaks in two branches over the over the central North Pacific.

The positive phase of SCA is associated with positive anomalies in the 500-hPa geopotential height over Scandinavia and western Russia, while during the negative phase negative anomalies prevail over these regions. The structure of the EA pattern resembles NAO, and its positive phase is often interpreted as a southward shifted NAO[25]. The positive phase of EAWR is associated with positive 500-hPa height anomalies over Europe and northern China and negative anomalies over North Atlantic and north of the Caspian Sea. The positive phase of PEU is associated with positive geopotential anomalies over China and Mongolia and negative anomalies over the Arctic.

Previous studies have mostly focused on the sea ice extent and duration of the ice season with very little or no attention to the effects of large-scale atmospheric conditions on ice and snow thickness in the Baltic Sea. Hence, in this study we focus on sea ice and snow thickness in the Gulf of Bothnia, northern Baltic Sea, during 33 winters, 1980/1981—2012/2013. Our objectives are to find out (a) how sea ice and snow thickness in the Gulf of Bothnia are controlled by the combined effects of local air temperature and precipitation; (b) which large-scale circulation conditions, characterized by indices of AO, NAO, PDO, PNA, and ENSO, favour low/high temperatures and excessive/little snow fall/rain; and (c) if variations in weather, snow, and sea ice conditions in the Gulf of Bothnia are related, via large-scale atmospheric circulation, to the recent rapid changes in the Arctic sea ice cover.

2 Material and methods

2.1 Site of research and data

We focus on snow and sea ice thickness, which have been measured in Kemi (24.5°E, 65.7°N; Figure 1) once a week over 33 years (winters 1980/1981—2012/2013). In this study the ice season is defined as from 1 November to 30 April. The 33-year average sea ice and snow thicknesses were 46 and 13 cm, respectively. The 33-year averages for the annual maximum values were 73 cm for ice thickness and 26 cm for snow thickness. For comparison, we also used data on the seasonal maximum snow thickness measured on land in the vicinity of the sea ice observation site. The study site at Kemi is located in the land-fast ice zone, where the sea ice thickness is controlled by thermodynamics. In this paper we only address atmospheric forcing factors, but recognize that also the autumn heat content of the sea is important.

Meteorological observations were made at Kemi-Tornio airport some 20 km north of the snow and ice measurement site. Daily mean air temperature and daily accumulated total precipitation were used to calculate mean temperature and accumulated total precipitation for each winter. The total precipitation (P) consists of snowfall (S) and rain/sleet (R). A threshold temperature of 0.5°C was applied to estimate S and R from P[26]. The 33-year means of winter mean, minimum, and maximum air temperature were –6.6°C, –27.5°C, and 6.1°C, respectively. The 33-year mean total winter precipitation was 219 mm water equivalent (weq), of which 160 and 59 mm weq were snowfall and rain/sleet, respectively.

The monthly index values of AO, NAO, PNA, SCA, PEU, EA, and EAWR were taken from the NOAA Climate Prediction Centre (http://www.cpc.ncep.noaa.gov/products/precip/CWlink/ daily_ao_index/teleconnections.shtml and http://www.cpc.ncep.noaa.gov/data/teledoc/telecontents.shtml). The AO index was calculated as the leading empirical orthogonal function of monthly mean Northern Hemisphere mean-sea-level pressure anomalies poleward of 20°N[27]. The PNA, NAO, SCA, PEU, EA, and EAWR indices were calculated using the Rotated Principal Component Analysis[25]. The analysis was applied to monthly standardized 500-mb height anomalies poleward of 20°N. The EA and EAWR indices did not have any statistically significant correlations with our observations, and are therefore not further discussed.

The monthly PDO values were taken from the NOAA / University of Washington, Joint Institute for the Study of the Atmosphere and Ocean (http://jisao.washington.edu/pdo/PDO.latest). To quantify the El Nino—Southern Oscillation (ENSO), we used the Monthly Multivariate ENSO Index from the NOAA Earth System Research Laboratory (http://www.esrl.noaa.gov/psd/enso/ mei/table.html).

In addition to local observations at Kemi, we applied the ERA-Interim reanalysis[28] to calculate the area-averaged 2-m air temperature, sea-ice concentration, and accumulated values for total precipitation, snow fall and rain over the Gulf of Bothnia.

We also applied data on the sea ice area in the Arctic Ocean and its marginal seas, taken from the National Snow and Ice Data Center (http://nsidc.org/data/seaice_index/archives.html). The sea ice area is the sum of the area covered by sea ice, calculated on the basis of satellite remote sensing information of sea ice concentration.

2.2 Methods

Pearson's correlation coefficients (r) were calculated to study bilateral statistical relationships between variables. The stepwise multi-linear regression analysis[29] was applied to identify further statistical relationships. First, we studied how inter-annual variations in the observed snow and ice parameters (seasonal mean and maximum values) are related to inter-annual variations in air temperature (seasonal mean, minimum, and maximum) and precipitation (P, S and R). Second, we studied how variations in the large-scale indices AO, NAO, PDO, PNA, ENSO, SCA, and PEU are related to variations in the observed meteorological and snow/ice conditions in the Gulf of Bothnia. Finally, we studied the links (via large-scale atmospheric circulation) between the Arctic sea ice cover and meteorological and snow/ice

conditions in the Gulf of Bothnia.

We applied the Climate Reanalyzer software of the Climate Change Institute at the University of Maine, USA, to calculate and plot spatial distributions and correlations of meteorological and ice/snow variables.

3 Results

3.1 Local relationships in the Gulf of Bothnia

The statistical relationships between the local weather forcing factors (air temperature, P, S, R) and the snow and ice thickness observed in Kemi are summarized in Table 1. The seasonal average ice thickness (H_{iave}) is mainly dominated by the seasonal average air temperature (T_{ave}) followed by the seasonal minimum air temperature (T_{min}). For seasonal maximum ice thickness (H_{imax}), also the total precipitation gives a positive impact, but its statistical significance is small; an r value of 0.75 (instead of 0.77) would be achieved without P included in the equation. The weak or no effect of precipitation variables on ice thickness is due to their compensating effects. A positive contribution to ice thickness may result from two processes: (1) heavy snowfall in early winter, when the ice is still thin, often causes snow-ice formation via sea water flooding and refreezing[30-31], and (2) heavy precipitation (liquid and solid) provides a large source for superimposed ice formation. After percolation to snow-ice interface, rain water refreezes to superimposed ice all through winter and spring, whereas accumulated snow refreezes to superimposed ice during the spring melt period, as demonstrated by observations[32] and model experiments[20] for the Baltic Sea. A negative contribution to ice thickness also results from two processes: (1) the role of snowfall as an insulator, reducing ice growth, and (2) the effect of rain in reducing the surface albedo, thus enhancing ice melt. The positive and negative effects seem to compensate each other, keeping the net effect of total precipitation very small (in the case of H_{imax}) or indistinguishable (in the case of H_{iave}).

Table 1 Multiple-linear regression equations for snow and ice thickness in Kemi as explained by the combined effects of air temperatures and precipitation variables. The explaining variables are written in the order of their statistical significance for the equation (strongest factors first). *rmse* denotes the root-mean-squared error; see the text for definitions of other symbols. The ice and snow thicknesses are in cm, the air temperatures in Kelvins and precipitation variables in mm weq

Regression equation	r	*rmse*	p	Regression equation	r	*rmse*	p
$H_{iave} = -2.3T_{ave} - 0.39T_{min} + 739$	0.71	5.9	$8.6e^{-5}$	$H_{smax} = -2.5T_{ave} + 0.09S - 0.07R + 683$	0.67	7.2	$1.7e^{-3}$
$H_{imax} = -1.5T_{min} - 2.2T_{ave} + 0.03P + 1003$	0.77	8.4	$5.3e^{-5}$	$H_{smaxL} = 0.17S - 0.17R - 2.5T_{ave} + 703$	0.73	9.6	$1.7e^{-4}$
$H_{save} = -1.5T_{ave} - 0.05R + 0.03S + 415$	0.67	4.5	$1.5e^{-3}$				

The seasonal mean and maximum snow thicknesses (H_{save} and H_{smax}, respectively) are affected by T_{ave}, R, and S (Table 1). A low T_{ave} contributes positively to H_{save} as there is less snow melt during a cold winter. S naturally increases the snow thickness, whereas R reduces it. Rain causes snow metamorphism, increasing the snow density and, accordingly, reducing the layer thickness. Further, the snow albedo is reduced by rain[33], which enhances the spring melt. Unlike H_{save}, H_{smax} is more strongly related to S than to R. This we interpret resulting from the strong effects of major individual snow fall events on H_{smax}.

It is noteworthy that the maximum snow thickness on land (H_{smaxL}) is more directly affected by precipitation (S and R) than by T_{ave} (Table 1). Compared to snow accumulation on sea ice, the snow accumulation on land is a more direct result of precipitation, as there is no mass transformation with the underlying soil. In the case of snow on sea ice, the thermodynamic processes of mass transformation (snow-ice and superimposed ice formation) make H_{smax} more sensitive to temperature.

Wind speed did not have any statistically significant relationships with the observed inter-annual variations in ice and snow thickness.

The measurement station in Kemi well represents the land-fast ice zone in the Gulf of Bothnia, but does not equally well represent the drift ice zone, where sea ice thickness is to some extent also affected by ice dynamics via ridging and rafting. The seasonal mean air temperature measured at Kemi-Tornio airport correlates, however, very well with the ERA-Interim based area-averaged 2-m air temperature over the Gulf of Bothnia ($r = 0.93$) and with the seasonal maximum ice extent in the whole Baltic Sea ($r = -0.84$), i.e. in a scale of the order of 1 000 km.

3.2 Relationships between large-scale indices and weather and ice conditions in the Gulf of Bothnia

It is well known that air temperatures in Northern Europe are strongly affected by NAO and AO (see the Introduction). This relationship for our study period (November—April in 1980/1981—2012/2013) is illustrated in Figure 2; the maximum effects of AO and NAO are felt within and around our study region, with the correlation coefficient (r) of approximately 0.6 for AO and 0.4—0.5 for NAO. The PDO and PNA indices are negatively correlated with 2-m air temperature, and for PDO the magnitude of r is approximately equally high as for NAO, but for PNA it is lower. SCA, ENSO and PEU have near-zero correlations in our study region of Kemi and the Gulf of Bothnia, but SCA has large areas of significant positive and negative correlations in the surrounding regions (Figure 2).

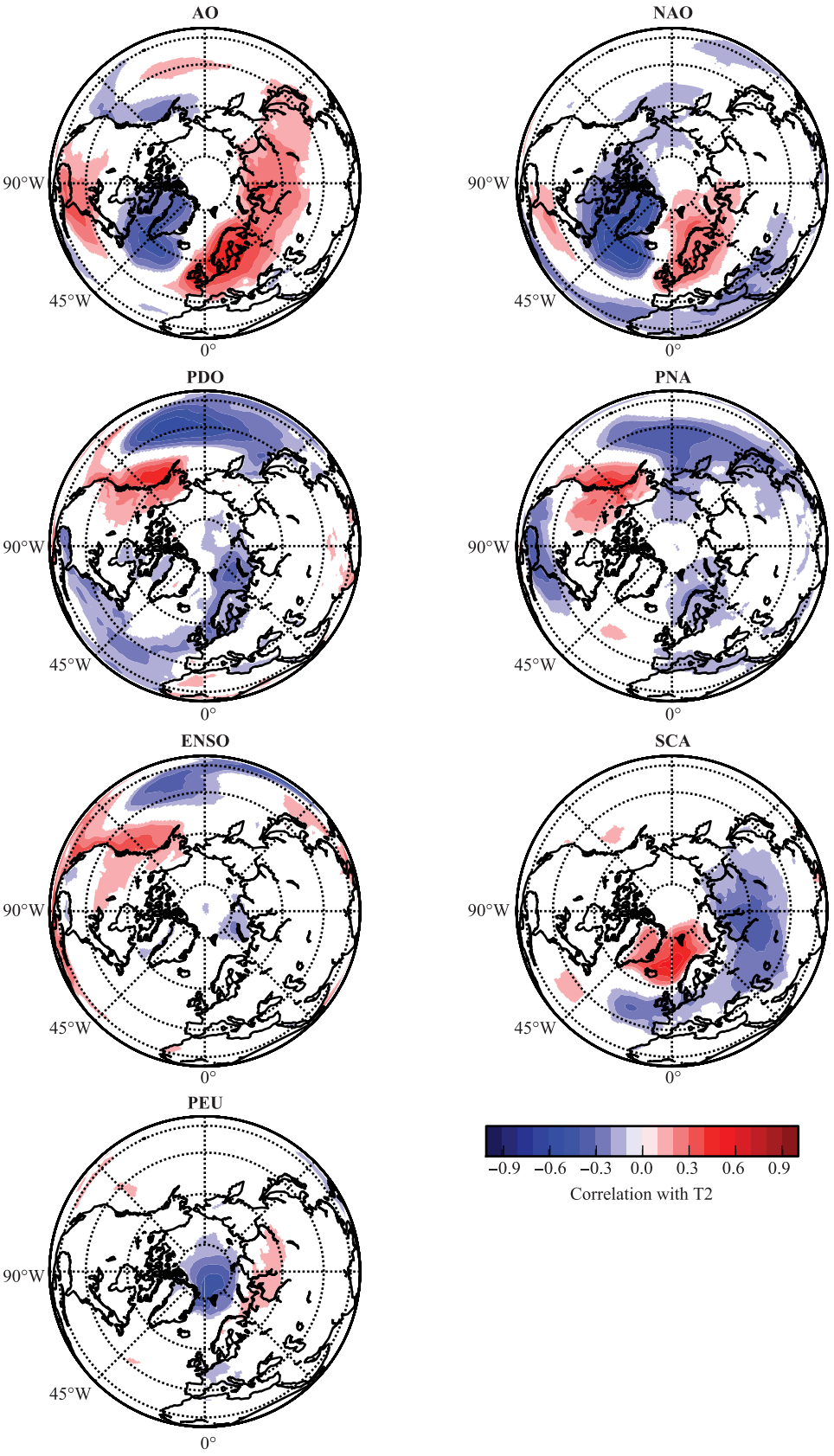

Figure 2 Correlation coefficient between 2-m air temperature and AO, NAO (principal component), PDO, PNA, ENSO, SCA, and PEU in November—April in 1980/1981—2012/2013. Areas where the Pearson correlation coefficient differs from zero at least at the 95% probability are plotted.

The correlation patterns for AO and NAO resemble each other, as do the patterns for PDO and PNA. This is not surprising, as some of the indices correlate mutually (p <0.05): AO positively with NAO (r = 0.79) and negatively with SCA (r = –0.71), PDO (r = –0.45) and PNA (r = –0.40); NAO negatively with SCA (r = –0.44); PDO positively with PNA (r = 0.63), ENSO (r = 0.55), and SCA (0.37); and PNA positively with ENSO (r = 0.61) (see the time series in Figure 3).

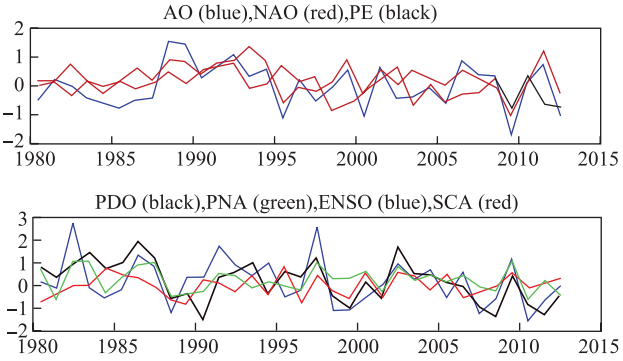

Figure 3 Time series of the monthly mean AO, NAO, PEU, PDO, PNA, ENSO, and SCA indices.

Next we shift our focus to our observations at Kemi and the ERA-Interim results for area-averaged variables over the Gulf of Bothnia for November—April in 1980/1981—2012/2013. Statistically significant bilateral correlations were found between the large-scale indices and the following variables: area-averages of winter mean air temperature (T_{GB}), precipitation (P_{GB}), and sea-ice concentration (SIC_{GB}) over the Gulf of Bothnia, winters means of air temperature (T_K), ice thickness (Hi_K), and snow thickness (Hs_K) in Kemi, as well as accumulated total precipitation (P_K), snow fall (S_K), and rain (R_K) in Kemi. The results are summarized in Table 2. It is noteworthy that PDO has more and stronger correlations with meteorological and snow/ice variables in the Gulf of Bothnia than NAO. Considering all the variables studied, PDO appears as important as AO. SCA is important for the area-averaged temperature and precipitation over the Gulf of Bothnia, and PEU correlates with precipitation and rain (Table 2). The roles of AO, NAO and, to some extent, SCA and PEU in the Baltic Sea and Northern Europe are well known, but the effect of PDO has not received much attention so far.

It is evident that the weather and snow/ice conditions in the Gulf of Bothnia are not affected by a single large-scale circulation index at a time. Hence, we carried out multiple regression analyses to study their combined effects. In the case of seven variables, T_{GB}, T_K, P_{GB}, P_K, S_K, R_{GB}, and SIC_{GB}, a combination of two or three large-scale indices yielded a better degree of explanation than a single index (Table 3). The strong statistical relationships with PDO are evident; it is the most important term in five equations and the second-most important term in one equation. AO is the most important term in the equation for T_{GB} and SCA in the equation for P_{GB}. It is noteworthy that although PNA and ENSO did not have any statistically significant bilateral correlations with the temperature, precipitation and snow/ice variables in the Gulf of Bothnia, they improve the degree of explanation when included in the multiple regression equations. PNA is present in four of the seven equations, improving the degree

Table 2 Correlation coefficients between large-scale indices (AO, NAO, PDO, SCA, and PEU) and local/regional variables T_{GB}, T_K, P_K, S_K, R_K Hi_K, Hs_K, and SIC_{GB}. See the text for definition of symbols. The winter mean and accumulated values are calculated for the November—April period. Correlation coefficients significant at confidence level $p < 0.01$ are marked as bold, whereas the other values shown are significant at $p < 0.05$

	T_{GB}	T_K	P_{GB}	P_K	S_K	R_K	Hi_K	Hs_K	SIC_{GB}
AO	**0.63**	**0.57**		0.39	0.36			–0.35	–0.38
NAO	**0.45**	**0.45**		0.35			–0.43		
PDO	**–0.54**	**–0.52**		**–0.46**	–0.38	–0.40		0.39	**0.48**
SCA	**–0.51**		**–0.54**						
PEU			–0.35	–0.41		–0.39			

Table 3 Multiple regression equations for air temperature, accumulated precipitation, accumulated snow fall, and sea ice concentration, as explained by the combined effects of large-scale indices. The indices are written in the order of their statistical significance for the equation. See the text for definitions of symbols. The air temperatures are in Kelvins, precipitation variables in mm weq, and sea ice concentration in percentages

Multiple regression equation	r	$rmse$	p	Multiple regression equation	r	$rmse$	p
T_{GB} = 1.24AO – 1.21PDO + 1.88PNA – 271.7	0.82	1.0	2×10^{-7}	S_K = –38.6PDO + 48.0PNA – 156	0.55	43	5×10^{-3}
T_K = –1.31PDO + 1.19AO + 1.85PNA – 266.4	0.75	1.3	2×10^{-5}	R_K = –16.7PDO – 30.9PEU + 61	0.52	39	9×10^{-3}
P_{GB} = –9.08SCA – 6.09PEU + 47	0.66	6	2×10^{-4}	SIC_{GB} = 9.94PDO – 5.4ENSO + 29	0.61	10	2×10^{-3}
P_K = –65.6PDO + 68.5PNA + 216	0.58	65	2×10^{-3}				

of explanation that AO and PDO provide for T_{GB} and T_K, and the one that PDO provides for P_K and S_K. The inter-annual variability of precipitation in the Gulf of Bothnia is best explained by the combined effects of SCA and PEU, and the variability of sea ice concentration by PDO and ENSO. The strongest relationships based on multiple regression analyses are illustrated in Figure 4.

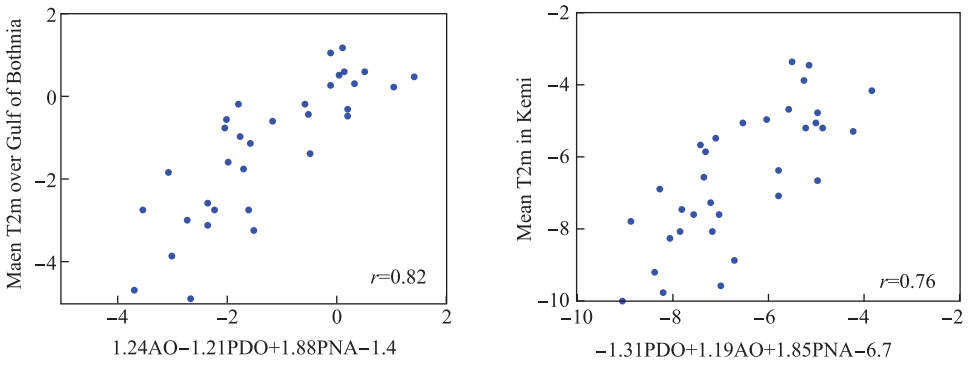

Figure 4 The combined effect of AO, PDO, and PNA on T_{GB} (**a**) and T_K (**b**) on the basis of the multiple regression analysis.

To better understand how the combined effects of AO, PDO, and PNA are related to large-scale wind field over the Gulf of Bothnia, we present in Figure 5 the December—February mean 500 hPa geopotential height maps for three winters when the parameter C_{TGB} = 1.24AO–1.21PDO + 1.88PNA–271.7 reached its highest values (1999/2000, 2006/2007, and 2011/2012) and for three winters when it reached its lowest values (1983/1984, 1995/1996, and 2012/2013). We see from Figure 5 that winters with a high C_{TGB} are associated with a low 500 hPa geopotential (lower than 5 280 m in all three winters) and, except in winter 2011/2012, a high geopotential gradient over the Gulf of Bothnia. These are related to strong winds, a high cyclone activity, and advection of warm marine air masses from the North Atlantic. These conditions favour high air temperatures over the Gulf of Bothnia. In the winters with a low C_{TGB} the 500 hPa geopotentials over the Gulf of Bothnia were higher (always more than 5 270 m and in 1995/1996 and 2012/2013 more than 5 340 m) and the gradients were weak, except in 1983/1984. These were associated with a high surface pressure, reduced cloud cover, and weaker westerly winds than in the winters with a high C_{TGB}.

Accordingly, in the period studied the variability of C_{TGB} was associated with large-scale flow patterns basically similar to those associated with the variability of AO and NAO. This raises the question if PDO has causal effects on weather over the Gulf of Bothnia, or if the statistical relationships only reflect PDO's statistical links with AO (r = –0.45). With a very low correlation with NAO (r = –0.17), PDO does not reflect linear causal effects of NAO variability on weather over the Gulf of Bothnia (in the 33-year period studied; over longer time scales the variability of PDO and NAO more resemble each other[34]). Although the statistical relationships detected between PDO and conditions in the Gulf of Bothnia may be partly related to the significant anti-correlation between PDO and AO, we note that the multiple regression equations presented in Table 3 would have clearly worse statistical scores (r, *rmse*, and p values), if only AO and PNA were included without PDO. Also, the bilateral correlations with precipitation and snow/ice variables are better for PDO than for AO (Table 1). We further compared the populations of winters when PDO and AO belonged to the highest and lowest 30% of their values during the study period (ten winters in each group). If the correlations between PDO and the Gulf of Bothnia variables would mostly reflect PDO's statistical links with AO, the winters with a high PDO and the winters with a low AO should be mostly the same winters, but only five (50%) of the winters were the same. The same was true for the winters with a low PDO and high AO: only five winters were the same.

We found out, however, that the correlations between PDO and air temperature and precipitation in the Gulf of Bothnia were unstable. A record of meteorological data since 1950 was available from Oulunsalo, along the coast of the Gulf of Bothnia some 100 km south of Kemi. During this period, the correlation between PDO and air temperature was only –0.24 (compared to –0.52 for Kemi since 1980/1981) and the one between PDO and precipitation was 0.04 (compared to –0.46).

Altogether, the results suggests that during 1980/1882—2012/2013 there was some causal teleconnection from the North Pacific to the Gulf of Bothnia (and probably to many other regions too).

3.3 Links to Arctic sea ice cover

Here we present simple statistical analyses on the observed relationships between the Arctic sea ice area and weather and snow/ice conditions in the Gulf of Bothnia (Table 4). The total precipitation and rain accumulated in Kemi in November—April period had a significant correlation with the Pan-Arctic sea ice area (including the Arctic Ocean and

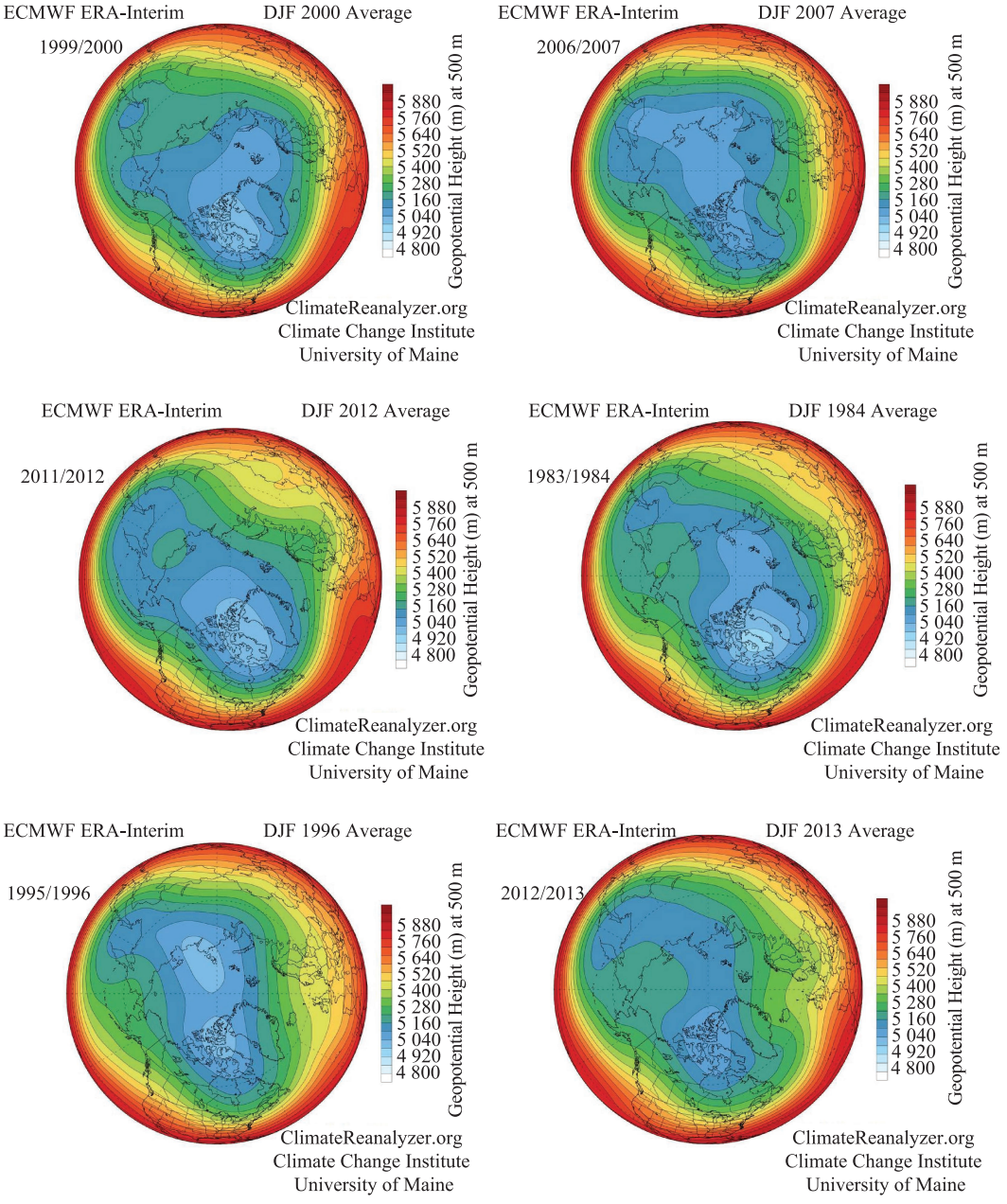

Figure 5 December——February mean 500 hPa geopotential height maps for three winters with highest and lowest values of parameter C_{TGB} = 1.24AO – 1.21PDO + 1.88PNA – 271.7.

marginal seas) in September, October, and November and, separately, with November sea ice area in the Barents and Kara seas. Less sea ice area in the Arctic was associated with more total precipitation and rain in Kemi. Significant correlations were detected neither for the accumulated snow fall in Kemi nor for any of the precipitation variables averaged over the Gulf of Bothnia. The latter may be related to the worse accuracy of the averaged values, based on ERA-Interim reanalysis instead of in-situ observation.

In addition to the statistically significant results reported in Table 4, it is interesting to note that variations in October—November sea ice area as far as in the Sea of Okhotsk have

Table 4 Statistically significant correlation coefficients between Arctic sea ice area and precipitation variables (total precipitation and snow fall) in Kemi. The values significant at $p < 0.01$ are marked as bold

Arctic sea ice variable	r for P_K	r for R_K
Arctic sea ice area in September	**–0.46**	**–0.50**
Arctic sea ice area in October	**–0.43**	**–0.48**
Arctic sea ice area in November	–0.38	**–0.45**
Barents–Kara Sea ice area–in November	**–0.43**	**–0.49**

almost significant correlations with the November–April mean air temperature over the Gulf of Bothnia ($r = –0.30$, $p = 0.09$), accumulated precipitation in Kemi ($r = –0.31$, $p = 0.08$), and maximum sea ice thickness in Kemi ($r = 0.30$, $p = 0.08$). The Arctic sea ice area did not correlate with air temperature, ice thickness, snow thickness, and sea ice concentration in the Gulf of Bothnia or Kemi. This was the case for the Pan-Arctic sea ice area and that in the Arctic Ocean and any of the marginal seas. The Pan-Arctic sea ice area had, however, an almost significant correlation with the maximum ice thickness in Kemi ($r = 0.33$, $p = 0.06$).

4 Discussion and conclusions

During winters 1980/1981—2012/2013, inter-annual variations in the winter air temperature, accumulated total precipitation, snow fall, and rain, as well as ice and snow thickness and ice concentration in the Gulf of Bothnia were statistically related to inter-annual variations in PDO, AO, NAO, SCA and PEU. The relationships were stronger with PDO than with NAO, SCA and PEU, and approximately equally strong with PDO and AO. The accumulated rain in Kemi and sea ice concentration in the Gulf of Bothnia were, however, better correlated with PDO than with AO. The strong relationships with PDO are a new finding. PDO was not even mentioned in the recent reviews of sea ice[13], physical oceanography[35], and weather and climate[22] in the Baltic Sea.

The factors controlling PDO variability are largely unknown, but the global importance of PDO is well demonstrated[34], while the physical mechanisms connecting the Pacific Ocean surface temperature fields and local weather in the Gulf of Bothnia are not well understood. Some possible mechanisms have been suggested. Due to regional cancellations of warming and cooling, PDO does not account for changes in global mean surface temperature, but is related to mean sea level pressure variability, with signals from the Pacific across the central Arctic to Europe[34]. The stratosphere probably plays an important role in this teleconnection[36]. Another pathway that may link the Pacific and Northern Europe is via mid-latitudes, proposed by Zhao et al.[37]. Reduced sea ice in the Bering and Okhotsk seas increases the regional sea surface temperatures, which according to Trenberth and Fasullo[34] is related to a positive phase of PDO. The sea surface temperatures anomalies generate an eastward propagating planetary wave, resulting in an anomalous high and less precipitation in Europe[37]. This mechanism is in accordance with our results: a negative correlation between PDO and Kemi/Gulf of Bothnia temperature and precipitation variables (Tables 2 and 3).

It is noteworthy that the correlations between PDO and conditions over the Gulf of Bothnia were not persistently significant (Section 3.2). Also previous studies have suggested that the linkages between the Pacific and Atlantic vary in time: during our study period PDO and NAO did not correlate, but over longer time periods the variability of PDO and NAO more resemble each other[34].

For area-averaged precipitation over the Gulf of Bothnia, SCA was the most important large-scale index. The combined effect of SCA and PEU yielded a rather high correlation and a particularly small root-mean-squared error. Also PNA and ENSO had statistical connections with the conditions in the Gulf of Bothnia, although not significant bilateral correlations. It is noteworthy that the inter-annual variability of sea ice concentration in the Gulf of Bothnia was statistically best explained by the combined effects of PDO and ENSO. The influence of ENSO on sea ice in the Baltic Sea has been suggested already by Jevrejeva et al.[9]. The physical mechanisms of this teleconnection are not well understood but, in general, ENSO is regarded as the most important driver of natural variability of the global mean surface temperature[24].

Rain and total precipitation accumulated in November—April in Kemi, the Gulf of Bothnia, are statistically related with Arctic sea ice cover in September—November. A reduced autumn sea ice, in the all Arctic and in the Barents/Kara seas alone, is related to increased rain and total precipitation in the following winter. This is understandable, as more open ocean in autumn is supposed to increase evaporation. Also previous studies have suggested that reduction of Arctic sea ice cover may yield increase in precipitation in certain mid-latitude locations. These include the British Isles, Central Europe, and Southern Scandinavia[38], Mediterranean[39], and parts of China[37, 40-42]. However, the positive precipitation anomaly that Screen[38] associated with Arctic sea ice decline did not reach the Gulf of Bothnia but occurred further southwest. During our study period, the Arctic sea ice cover did not have any significant correlations with air temperature and sea ice conditions in the Gulf of Bothnia. This may be due to the dominating effects of PDO and AO on air temperature and sea ice conditions in our study region. The variability of PDO and AO is not dominated by variability of the Arctic sea ice cover, although there seems to be some effect on AO[15]. The tendency of the Arctic sea ice decline to cause a negative phase of AO may be partly compensated by the fact that when there is less sea ice in the Barents Sea, the cases of cold-air advection from the north are less cold in the Gulf of Bothnia than in conditions with a lot of sea ice in the north.

Although our study did not reveal any statistically significant correlations with the EA and EAWR indices, we note that in individual months EA may be very important in explaining the north/southward shifts of NAO's centers of action and related effects on air temperature in Europe[43].

Although the links with the sea ice area in the Sea of Okhotsk were not significant at $P < 0.05$, the results were interesting. Also several previous studies have detected links between the Sea of Okhotsk ice cover and weather conditions in remote areas. The proposed physical mechanisms have been related to sea ice loss and its effects on increased cyclogenesis and strengthening of the North Pacific storm track[38, 44] and generation of stationary patterns of planetary waves (so-called wave trains)[37, 45-46].

Our findings present a call for more studies to better understand the physical mechanisms responsible for the hemispheric-scale teleconnections.

Acknowledgments This work is supported by the Academy of Finland (Grant no. 259537). The Young Scientists Fund of National Natural Science Foundation of China (Grant no. 41206186) is acknowledged. Figures 1, 2, and 5 were prepared applying the Climate Reanalyzer, which is an initiative of the Climate Change Institute at the University of Maine, USA. We thank three anonymous reviewers for their valuable comments on the manuscript.

References

1 Leppäranta M, Makkonen L, Palosuo E, et al. Geophysics of snow and ice in Finland during the 1900s. Geophysica, 2001, 31: 261-285.
2 Sass A F. Untersuchungen über die Eisbedeckung des Meeres and den Küsten der Inseln Ösel und Moon. Bulletin de l'Academie Imperiale des Sciences de St. Petersbourg, 1866, 9: 145–188.
3 Seinä A, Palosuo E. The classification of the maximum annual extent of ice cover in the Baltic Sea 1720–1995. Meri, Report Series of the Finnish Institute of Marine Research, 1996, 20: 79–910.
4 Koslowski G, Loewe P. The western Baltic Sea ice seasons in terms of mass-related severity index 1879–1992. Tellus, 1994, 46A: 66–74.
5 Omstedt A, Chen D. Influence of atmospheric circulation on the maximum ice extent in the Baltic Sea. Journal of Geophysical Research, 2001, 106: 4493–4500.
6 Jevrejeva S, Moore J C. Singular Spectrum Analysis of Baltic Sea ice conditions and large-scale atmospheric patterns since 1708. Journal of Geophysical Research, 2001, 28: 4503–4506.
7 Yoo J C, D'Odorico P. Trends and fluctuations in the dates of ice break-up of lakes and rivers in Northern Europe: the effect of the North Atlantic Oscillation. Journal of Hydrology, 2002, 268: 100–112.
8 Meier H E M, Kauker F. Simulating Baltic Sea climate for the period 1902–1998 with the Rossby Centre coupled ice–ocean model. Reports Oceanography, SMHI, Norrköping, Sweden, 2002, 30: 111.
9 Jevrejeva S, Moore J C, Grinsted A. Influence of the Arctic Oscillation and El Nino-Southern Oscillation (ENSO) on ice conditions in the Baltic Sea: the wavelet approach. Journal of Geophysical Research, 2003, 108: doi:10.1029/2003JD003417.
10 Chen D, Li X. Scale-dependent relationship between maximum ice extent in the Baltic Sea and atmospheric circulation. Global and Planetary Change, 2004, 41: 275–283.
11 Omstedt A, Pettersen C, Rodhe J. et al. Baltic Sea climate: 200 yr of data on air temperature, sea level variation, ice cover and atmospheric circulation. Climate Research, 2004, 25: 205–216.
12 Jaagus J. Trends in sea ice conditions on the Baltic Sea near the Estonian coast during the period 1949/50–2003/04 and their relationships to large-scale atmospheric circulation. Boreal Environment Research, 2006, 11: 169–183.
13 Vihma T, Haapala J. Geophysics of sea ice in the Baltic Sea – a review. Progress in Oceanography, 2009, 80: 129–148, doi: 10.1016/j.pocean.2009.02.002.
14 Cohen J, Screen J A, Furtado J C, et al. Recent Arctic amplification and extreme mid-latitude weather. Nature Geoscience, 2014, 7: 627–637.
15 Vihma T. Effects of Arctic sea ice decline on weather and climate: a review. Surveys in Geophysics, 2014, 35: 1175–1214, doi 10.1007/s10712-014-9284-0.
16 Walsh J E. Intensified warming of the Arctic: causes and impacts on middle latitudes. Global and Planetary Change, 2014, 117: 52–63, doi:10.1016/j.gloplacha.2014.03.003.
17 Haapala J, Leppäranta M. Simulations of the ice season in the Baltic Sea, Tellus, 1996, 48A: 622–643.
18 Launiainen J, Cheng B. Modelling of ice thermodynamics in natural water bodies. Cold Regions Science and Technology, 1998, 27: 153–178.
19 Cheng B, Vihma T, Launiainen J. Modelling of the superimposed ice formation and sub-surface melting in the Baltic Sea. Geophysica, 2003, 39: 31–50.
20 Cheng B, Vihma T, Pirazzini R. et al. Modelling of superimposed ice formation during spring snowmelt period in the Baltic Sea. Annals in Glaciology, 2006, 44: 139–146.
21 Cheng B, Vihma T, Rontu L, et al. Evolution of snow and ice temperature, thickness and energy balance in Lake Orajärvi, northern Finland. Tellus, 2014, 66A: 21564, http://dx.doi.org/10.3402/tellusa.v66.21564.
22 Rutgersson A, Jaagus J, Schenk F, et al. Observed changes and variability of atmospheric parameters in the Baltic Sea region during the last 200 years. Climate Research, 2014, 61: 177–190, doi: 10.3354/cr01244.
23 Mantua, N J, Hare S R. The Pacific Decadal Oscillation, Journal of Oceanography, 2002, 58: 35–44, doi:10.1023/A:1015820616384.
24 Trenberth K E, Caron J M, Stepaniak D P, et al. The evolution of ENSO and global atmospheric surface temperatures. Journal of Geophysical Research, 2002, 107: 4065, doi:10.1029/2000JD000298.
25 Barnston A G, Livezey R E. Classification, seasonality and persistence of low-frequency atmospheric circulation patterns. Monthy Weather Review, 1987, 115: 1083–1126.
26 Yang Y, Leppäranta M, Cheng B, et al. Numerical modelling of snow and ice thickness in Lake Vanajavesi, Finland. Tellus, 2012, 64A: 17202, doi: 10.3402/tellusa.v64i0.17202.
27 Thompson D W J, Wallace J M. The Arctic Oscillation signature in the wintertime geopotential height and temperature fields. Geophysical Research Letters, 1998, 25: 1297–1300.
28 Dee D P, et al. The ERA-Interim reanalysis: configuration and performance of the data assimilation system, Quarterly Journal of the Royal Meteorological Society, 2011, 137: 656, doi:10.1002/qj.828.
29 Draper N R, Smith H. Applied Regression Analysis. Wiley-Intersci., Hoboken, N. J., 1998: 736 .
30 Kawamura T, Shirasawa K, Ishikawa N, et al. Time series observations of the structure and properties of brackish ice in the Gulf of Finland, the Baltic Sea. Annals of Glaciology, 2001, 33: 1–4.
31 Granskog M A, Kaartokallio H, Shirasawa K. Nutrient status of Baltic Sea ice: Evidence for control by snow-ice formation, ice permeability, and ice algae. Journal of Geophysical Research, 2003, 108: 3253, doi:10.1029/2002JC001386.
32 Granskog M, Vihma T, Pirazzini R et al. Superimposed ice formation and surface fluxes on sea ice during the spring melt-freeze period in the Baltic Sea. Journal of Glaciology, 2006, 52: 119–127.
33 Mazurkiewicz A B, Callery D G, McDonnell J J. Assessing the controls of the snow energy balance and water available for runoff in a rain-on-snow environment. Journal of Hydrology, 2008, 354: 1–14.
34 Trenberth K E, Fasullo J T. An apparent hiatus in global warming? Earth's Future, 2013, doi:10.1002/2013EF000165.
35 Omstedt A, Elken J, Lehmann A, et al. Progress in physical oceanography of the Baltic Sea during the 2003-2014 period. Progress in Oceanography, 2014, doi: http//dx.doi.org/10.1016/j.pocean.2014.08.010.
36 Ineson S, Scaife A A. The role of the stratosphere in the European climate response to El Nino. Nature Geoscience, 2009, 2: 32–36, doi:10.1038/ngeo381.

37 Zhao P, Zhang X, Zhou X, et al. The sea ice extent anomaly in the North Pacific and its impact on the East Asian summer monsoon rainfall. Journal of Climate, 2004, 17: 3434–3447.
38 Screen J A. Influence of Arctic sea ice on European summer precipitation. Environmental Research Letters, 2013, 8: 044015.
39 Grassi B, Redaelli G, Visconti G. Arctic sea-ice reduction and extreme climate events over the Mediterranean region. Journal of Climate, 2013, 26: 10101–10110, doi: http://dx.doi.org/10.1175/JCLI-D-12-00697.1.
40 Wu B, Zhang R, Wang B, et al. On the association between spring Arctic sea ice concentration and Chinese summer rainfall. Geophysical Research Letters, 2009, 36, L09501.
41 Guo D, Gao Y, Bethke I, et al. Mechanism on how the spring Arctic sea ice impacts the East Asian summer monsoon. Theoretical and Applied Climatology, 2013, 115:107–119, doi: 10.1007/s00704-013-0872-6.
42 Uotila P, Karpechko A, Vihma T. Links between Arctic sea ice and extreme summer precipitation in China: an alternative view. Advances in Polar Science, 2014, 25(4): 222–233.
43 Moore G W K, Renfrew I A. Cold European winters: interplay between the NAO and the East Atlantic mode. Atmospheric Science Letters, 2011, 13, doi:10.1002/asl.356.
44 Mesquita M D S, Hodges K I, Atkinson D A, et al. Sea-ice anomalies in the Sea of Okhotsk and the relationship with storm tracks in the Northern Hemisphere during winter. Tellus, 2011, 63A: 312–323.
45 Honda M, Yamazaki K, Tachibana Y, et al. Influence of Okhotsk sea-ice extent on atmospheric circulation. Geophysical Research Letters, 1996, 23: 3595–3598.
46 Honda M, Yamazaki K, Nakamura H, et al. Dynamic and thermodynamic characteristics of atmospheric response to anomalous sea-ice extent in the Sea of Okhotsk. Journal of Climate, 1999, 12: 3347–3358.